

## Passive Aerosol Sampler. Part II: Wind Tunnel Experiments

Jeff Wagner & David Leith

To cite this article: Jeff Wagner & David Leith (2001) Passive Aerosol Sampler. Part II: Wind Tunnel Experiments, *Aerosol Science & Technology*, 34:2, 193-201, DOI: [10.1080/027868201300034826](https://doi.org/10.1080/027868201300034826)

To link to this article: <https://doi.org/10.1080/027868201300034826>



Published online: 30 Nov 2010.



Submit your article to this journal [↗](#)



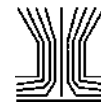
Article views: 543



View related articles [↗](#)



Citing articles: 37 View citing articles [↗](#)



# Passive Aerosol Sampler. Part II: Wind Tunnel Experiments

Jeff Wagner and David Leith

University of North Carolina, Department of Environmental Sciences and Engineering,  
Chapel Hill, North Carolina

Wind tunnel experiments have been performed on a passive aerosol sampler. The sampler estimates average concentrations and size distributions using a deposition velocity model and the measured particle flux to the sampler. The small-scale wind tunnel incorporated a high-output aerosol generator that produced nonvolatile, polydisperse particles. An eight-stage impactor was connected to the tunnel with an isoaxial, isokinetic probe and was equipped with polycarbonate-membrane substrates saturated with oleic acid to minimize particle bounce. Before performing experiments, the tunnel's test section was characterized. Aerosol concentrations were determined to have a CV < 6%. The friction velocity, an index of turbulence, was found to range from 0.09 to 0.25 m/s for wind speeds of 1.5 to 5 m/s. The empirical portion of the deposition velocity model,  $\gamma_m$ , was determined as a function of particle size by minimizing the sum-of-squares difference between impactor and passive sampler across all size bins and all experiments. The relatively simple correlation is a function of the particle Reynolds number only. Precision was assessed by running three passive samplers simultaneously in each experiment. The tests yielded  $CV_{PM2.5} = 18.1\%$  and  $CV_{PM10} = 32.2\%$ . ANOVA tests were conducted on accuracy and precision to see whether they depended on wind speed, relative humidity, or aerosol concentration, and accuracy was tested with respect to particle size. No significant trends were observed. Sensitivity analysis showed that the volume shape factor is the most important of the mass and shape conversion factors. If SEM is used, the passive sampler will exhibit some error when sampling volatile aerosols. Because concentrations fluctuate over time, long-term exposures measured by the passive sampler should be more accurate than conventional averages based on short-term samples.

## INTRODUCTION

The overall objective of this research is to develop a miniature passive aerosol sampler to estimate average size distributions and concentrations. The passive sampler monitors ambient, indoor, or occupational aerosols over periods of hours to weeks and

is about the size of a dime. During sampling, particles passively deposit on the collection surface. Scanning electron microscopy (SEM) or other microscopy techniques are then used to analyze the collected particles (Wagner and Leith 2001).

Mass size distributions are calculated by dividing the measured mass flux,  $F$ , by the deposition velocity,  $v_{dep}$ :

$$C = \frac{F}{v_{dep}} = \frac{F}{v_{amb}\gamma_m} \quad [1]$$

where  $C$  is the average mass concentration over the sampling period,  $v_{amb}$  is the ambient deposition velocity, and  $\gamma_m$  is the mesh factor. All are calculated as a function of aerodynamic diameter,  $d_a$ . Standard measures of airborne particulate levels such as PM<sub>2.5</sub> and PM<sub>10</sub> (mass concentration of particles with aerodynamic diameters <2.5  $\mu\text{m}$  and 10  $\mu\text{m}$ , respectively) can be calculated by integrating  $C$  over the appropriate particle sizes.

A special wind tunnel was designed and built to test the passive sampler. The wind tunnel tests were used to determine  $\gamma_m$  under different wind conditions and to determine the precision of the passive sampler.

This paper begins by describing the rationale for these tests and the design of the wind tunnel. Next, the characterization of the wind tunnel's concentration and flow fields is described. Methods, results, and discussion of the passive sampler tests follow. The paper concludes with sensitivity and uncertainty analyses.

## WIND TUNNEL DESIGN

### Test Objectives and Rationale

The objectives of the wind tunnel tests were to determine  $\gamma_m$  under different wind conditions and to determine the precision of the passive sampler. The empirical expression for  $\gamma_m$  was determined by fitting the size distribution results of the passive sampler to those of an active, mass-based sampler. Because "accuracy" has been defined with respect to the reference sampler, an effort was made to reduce the reference sampler's uncertainties as much as possible. Precision was assessed by testing

Received 13 April 1999; accepted 10 December 1999.

Address correspondence to Jeff Wagner, Department of Environmental Sciences and Engineering, CB#7400, Rosenau Hall, Chapel Hill, NC 27599. E-mail: jr.wagner@lbl.gov

three passive samplers simultaneously. A secondary objective was to determine if  $\gamma_m$  was dependent on the relative humidity or aerosol concentration.

Although many approaches are possible when testing a sampler, a decision was made to test under defined, stable conditions. The effect of more realistic, fluctuating conditions will be assessed separately with field tests. Experiments were designed for a range of constant wind speeds and an aerosol with known properties. The two major variables of the experiments were then wind speed and particle size.

### **Unique Features of the Wind Tunnel**

Because testing of the passive sampler required some unique conditions, a special wind tunnel was designed and built.

Several criteria had to be met for the aerosol generator and test aerosol. For one, the passive sampler is designed to sample over a period of weeks. To scale down experiment times so that they were on the order of hours, it was necessary to scale up the aerosol concentrations accordingly. Thus an aerosol generator capable of producing sustained high concentrations was needed, as well as a large quantity of particulate matter. Because analyses were conducted under vacuum with an SEM, a nonvolatile aerosol was needed. Finally, the test aerosol had to be polydisperse, with a portion in the submicron range.

To satisfy these criteria, a HEART high-output nebulizer (Westmed, Inc., Tuscon, AZ) was used to disperse continuously a slurry of distilled water and a manufactured SiO<sub>2</sub> dust (CERAC, Milwaukee, WI). A Kr-85 neutralizer (Model 3054, TSI Inc., St. Paul, MN) was used to neutralize the aerosol immediately downstream of the nebulizer. Because the output of the nebulizer was 12 LPM, or less than one tenth of the neutralizer's maximum recommended flow rate, the aerosol was assumed to be fully neutralized. The nebulized SiO<sub>2</sub> dust had a size range of approximately (0.6–9)  $\mu\text{m}$ , and an average of 13 g SiO<sub>2</sub>/200 ml H<sub>2</sub>O was nebulized per experiment. The original size distribution of the SiO<sub>2</sub> was slightly undesirable in that it had too many coarse particles. The distribution was improved by injecting the nebulized aerosol near the bottom of one end of the tunnel, removing many of the coarse particles as the aerosol traveled toward the test section at the other end. Using this apparatus, concentrations of up to 7.4 mg/m<sup>3</sup> were maintained in the tunnel's test section for 2–7 h, with an average mass median aerodynamic diameter of 2.5  $\mu\text{m}$  and geometric standard deviation of 1.8.

To achieve high concentrations at wind speeds of up to 5 m/s, the wind tunnel was built with a small cross-section (50 × 100) mm. Because the passive samplers are also quite small, placing three passive samplers side by side in the tunnel was feasible. Using a smaller cross section also made it easier to maintain a uniform concentration profile than would be possible with a conventional, larger wind tunnel (Ramachandran et al. 1998).

The reference sampler was an eight-stage Andersen cascade impactor (Andersen Instruments Inc., Smyrna, GA) with size cuts between (0.43–9)  $\mu\text{m}$  and a 10  $\mu\text{m}$  preseparator. To min-

imize particle bounce, a 77 mm polycarbonate membrane substrate with 5.0  $\mu\text{m}$  pore size was placed on each impactor stage and saturated with 20  $\mu\text{L}$  oleic acid. The substrates were trimmed down from 90 mm Isopore filters (Millipore, Bedford, MA). This approach was based on the work of Turner and Hering (1987). The impactor was equipped with a probe mounted isoaxially with the tunnel flow. Interchangeable probe inlets were used to sample isokinetically at each wind speed.

### **Overview of Wind Tunnel**

A schematic of the wind tunnel is shown in Figure 1. The straight section of the tunnel was constructed of clear acrylic, had a rectangular cross section, and was 2.4 m long. Air was pulled through the straight section by two high-volume samplers (hivols) in parallel. Wind speeds in the tunnel were adjusted by variable transformers connected to the hivols and were monitored with a hot-film anemometer (Velocichck Model 8830, TSI Inc., St. Paul, MN).

Aerosol was injected at the bottom of the entrance to the tunnel. The aerosol then encountered turbulence screens at 51 and 56 cm downstream. The screens had wire spacings of 1.2 cm and 0.2 cm, respectively. The first screen was blocked across the bottom half to create a flow "hurdle." This feature enhanced particle mixing into the upper half of the tunnel cross section. After travelling the length of the straight section, the aerosol encountered the test section. There, three passive samplers were mounted side by side in a holder in the mid-plane of the tunnel. The samplers' collection surfaces were parallel to the flow, and the samplers were electrically grounded. The inlet to the impactor probe was mounted 6.5 cm behind the passive samplers, also in the mid-plane of the tunnel. Finally, the aerosol traveled around a 45° elbow through a filter holder and hivol manifold. The unit consisting of the hivol manifold, filter holder, and impactor apparatus was mounted on a wheeled cart that could be detached from the rest of the wind tunnel.

Aerosol concentrations in the wind tunnel were monitored qualitatively with one of two real-time optical aerosol monitors, either a DataRAM (MIE Inc., Billerica, MA) or DustTRAK (TSI Inc., St. Paul, MN). Relative humidity in the tunnel was monitored with a dew point hygrometer (Model 11-661, Fisher Scientific, Atlanta, GA).

## **WIND TUNNEL CHARACTERIZATION**

### **Spatial Uniformity of Aerosol**

A valid comparison between two samplers requires that both be exposed to comparable aerosols. Because the passive samplers were located 6.5 cm away from the impactor's probe inlet, establishing spatial uniformity in the test section was important. Spatial uniformity of the aerosol was characterized with an Aerosizer LD (API, Hadley, MA), a time-of-flight particle sizer. Aerosol measurements were taken at 18 points across two equal area 3 × 3 traverse planes (Figure 2). The first plane was located 3.2 cm upstream of the samplers, while the second

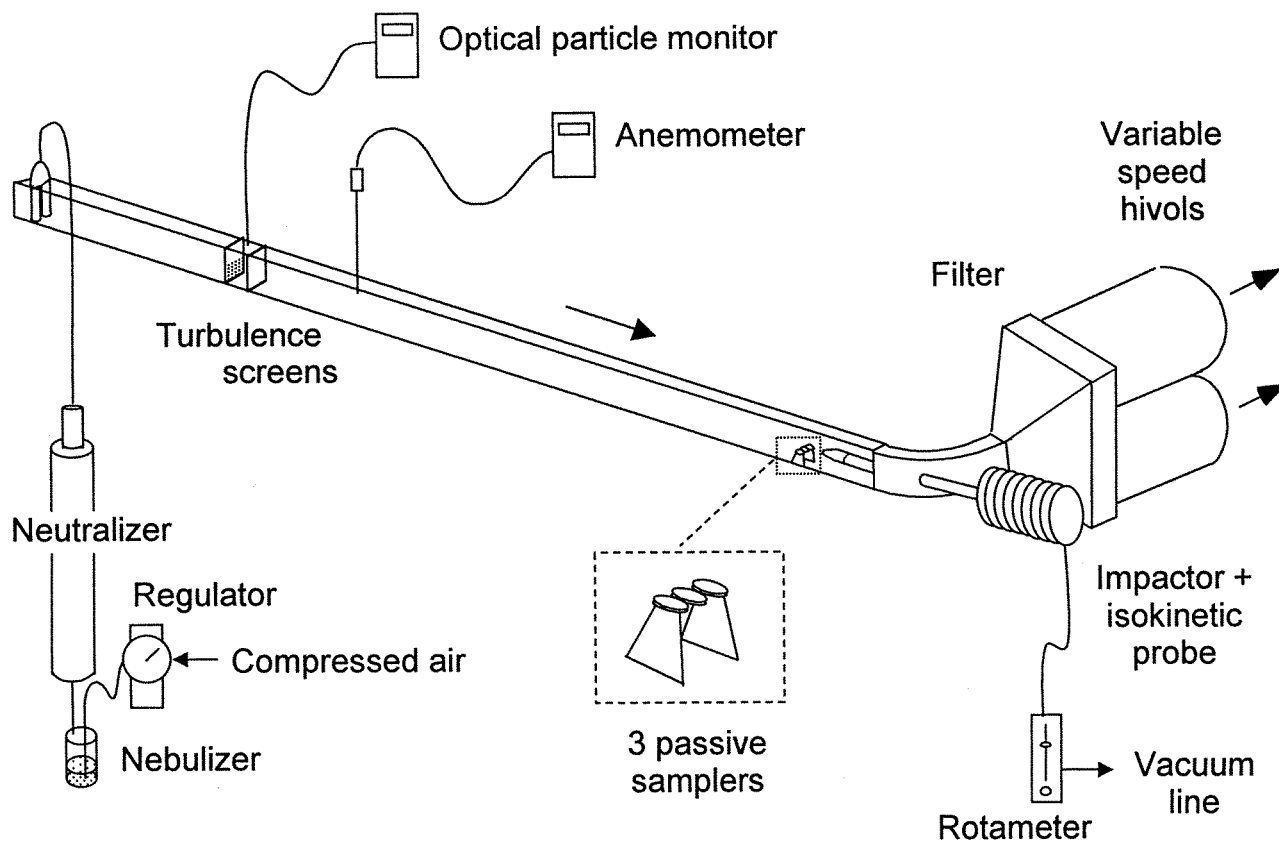


Figure 1. Wind tunnel for testing passive samplers.

plane was located between the passive samplers and the impactor probe, 2 cm downstream of the passive samplers. Three sets of replicates were performed at each location, for a total of 54 measurements. The aerosol used for these tests was a lactose aerosol with a measured aerodynamic size range of approximately  $0.2\text{--}4\ \mu\text{m}$  and a mass median aerodynamic diameter of  $1.0\ \mu\text{m}$ . Sampling was performed by inserting a small, grounded copper probe ( $7.5\ \text{cm}$  long,  $\text{ID} = 5\ \text{mm}$ ) into sampling ports on the side of the tunnel. The probe had a  $90^\circ$  elbow so that the inlet was parallel to the flow direction. The passive samplers were

mounted on the tunnel floor during these tests. Measurements were taken at the lowest tunnel wind speed used in the passive sampler experiments,  $u = 1.5\ \text{m/s}$ , to achieve a “worst case” mixing of the aerosol.

For total mass concentration, small but significant differences were found between positions and as a function of height above the tunnel floor. The coefficient of variation (CV) between positions was fairly low:  $\text{CV} = 5.6\%$ . In addition, only 28% of the 153 pairwise comparisons between positions showed significant differences. Average concentrations across the two traverse planes were not significantly different.

The diameter of average mass was also calculated for each measured size distribution. No significant differences were found between positions or with height. The CV between positions and all CVs within position were very low,  $<1\%$ .

A limitation of this characterization is that most measured particles had an aerodynamic diameter of  $d_a < 4\ \mu\text{m}$ . Larger particles could exhibit more spatial variability than described above, although approximately 70% of the aerosol mass in the passive sampler experiments described later was also  $<4\ \mu\text{m}$ . To further reduce the effects of any variability, the passive sampler mount was modified for subsequent experiments so that the samplers were at the same height as the impactor probe. Thus the aerosols measured by the passive samplers and the impactor were judged to be reasonably comparable and suitable for further work.

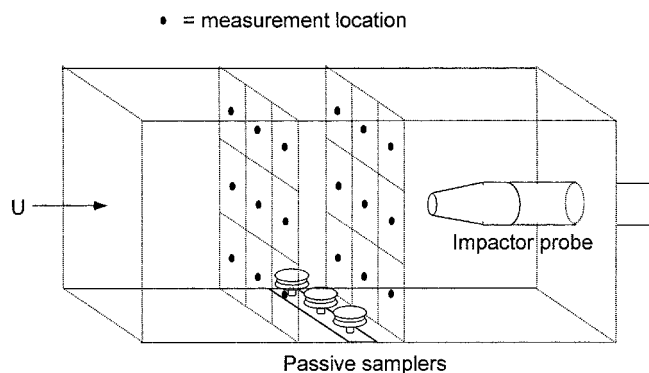


Figure 2. Traverses used for concentration uniformity measurements.

### Turbulence Characterization

Because the tunnel's reference sampler was active rather than passive, it was not appropriate to establish that both sampler types experienced comparable flow fields. Instead, each sampler type had different flow considerations. The impactor required isokinetic and isoaxial sampling conditions. At the start of each experiment, the velocity adjacent to the probe inlet was measured with a hot-film anemometer (Velocichck Model 8830, TSI, Inc., St. Paul, MN). The probe alignment and tunnel wind speed were then adjusted so that the tunnel velocity was equal in magnitude and direction to the probe inlet velocity.

For the passive sampler, it was necessary to characterize the friction velocity,  $u_*$ , in the test section. This parameter is an index of the turbulence and is required for development of the deposition velocity model. At each of the four experimental wind speeds, vertical velocity profiles were measured upstream of the passive samplers in the center of the tunnel cross section. Velocity profiles were measured with a platinum hot-film anemometer (Model 1240-20, TSI Inc., St. Paul, MN) and controller/signal processor (IFA-100 Intelligent Flow Analyzer, TSI Inc., St. Paul, MN). The anemometer was calibrated in a 0.20 m diameter flanged duct with an orifice meter.

Each velocity profile consisted of 6 pairs of replicate measurements of the mean streamwise component of the velocity. Because calculations showed that the flow was in the "hydraulically smooth" regime, an equation for the velocity profile in a smooth pipe was then adapted from Schlichting (1979):

$$u(y_{e\alpha}) = u_* \left[ 2.5 \ln \left( \frac{y_{e\alpha} u_*}{\nu} \right) + 5.5 \right], \quad [2]$$

where  $u(y_{e\alpha})$  is the wind speed at a distance  $y_{e\alpha}$  from the tunnel walls,  $\nu$  is the kinematic viscosity,  $y_{e\alpha} = (yD_h/H)$ ,  $y$  is the actual vertical distance,  $H$  is the vertical height of the tunnel,  $D_h = (4A/P_w)$  is the hydraulic diameter,  $A$  is the cross-sectional area of the tunnel, and  $P_w$  is the wetted perimeter of the tunnel. The concept of effective distance was used to account for the noncircular tunnel cross section.

By adjusting the value of  $u_*$ , Equation (2) could then be fitted to each vertical profile using the method of least squares. An example data fit is shown in Figure 3. This procedure was used to determine  $u_*$  empirically as a function of tunnel wind speed (Table 1). Although these  $u_*$  values are strictly valid for the center passive sampler only, they were assumed to represent adequately the turbulence near the left and right samplers as well. This assumption was supported by later experiments, which revealed no consistent variation in deposition across the tunnel cross section (see Results).

A regression analysis of the logarithms of  $u_*$  and the mean tunnel wind speed,  $U$ , yielded

$$u_* = (6.2 \times 10^{-2}) U^{0.88}. \quad [3]$$

For these experiments,  $\nu = 1.5 \times 10^{-5} \text{ m}^2/\text{s}$  and  $D_h = 0.07 \text{ m}$ . Using these values and an equation developed by Blasius for

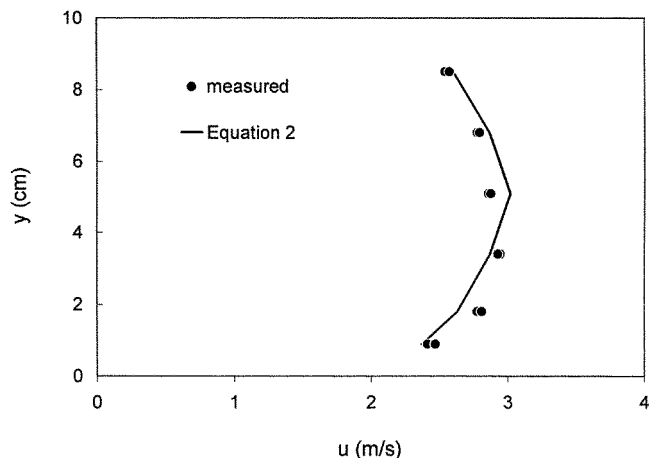


**Figure 3.** Fit of Equation (2) to a measured velocity profile. For this profile,  $u_{avg} = 2.7 \text{ m/s}$  and  $u_* = 0.15 \text{ m/s}$ .

pipe flow (cited in White (1994)), one obtains

$$u_* = U \left( \frac{0.316 Re_d^{-1/4}}{8} \right)^{1/2} = 0.2U \left( \frac{\nu}{D_h U} \right)^{1/8} \\ = (6.9 \times 10^{-2}) U^{0.875}, \quad [4]$$

where  $Re_d$  is the duct Reynolds number. By comparing Equations (3) and (4), one can see that the experimental result found in this study matches that predicted by theory extremely well.

## METHODS

### Experiment

To prepare the passive samplers for each experiment, four mesh caps, one plastic case, and a section of aluminum tape were cleaned with soap, water, and methanol. The meshes were further cleaned with a fine-haired brush and blasts of compressed air to clear the mesh holes of any debris. Spray mount adhesive was applied to the surfaces of four SEM stubs, and one 7 mm aluminum disc was placed in the center of each stub. After cleaning the discs with methanol, a mesh cap was placed onto each substrate and the samplers were closed inside their plastic case until the experiment began. The fourth passive sampler was used as a sampling blank.

**Table 1**

Results of wind tunnel turbulence measurements			
Nominal tunnel wind speed (m/s)	Velocity at probe inlet (m/s)	Mean wind speed, $U$ (m/s)	Friction velocity, $u_*$ (m/s)
1.5	1.6	1.5	0.09
3	2.9	2.7	0.15
4	3.9	3.7	0.20
5	5.0	4.9	0.25

Impactor concentrations were obtained gravimetrically with an analytical balance (Mettler Toledo Model AE200, Toledo, OH). Preweighing was conducted at least 1 h after applying oleic acid to the impactor substrates.

Duplicate experiments were run at  $u = 1.5, 3, 4,$  and  $5$  m/s. Concentrations and relative humidities varied randomly between experiments. Relative humidity (RH) and temperature were recorded at the start and end of each experiment with the nebulizer running.

At the end of each experiment, the three passive samplers were returned to their plastic case to stop sampling.

### Passive Sampler Analysis

The general analysis procedure is described elsewhere (Wagner and Leith 2001); additional methods and parameters used in the wind tunnel experiments are presented here. Before obtaining images with a Cambridge S-200 SEM (Leo Inc., Fomwood, NY), each passive sampler substrate was sputter-coated with a 60/40% gold/palladium alloy to enhance conductivity and resolution. Counts per area as a function of particle size were obtained for particles with  $d_p > 0.1 \mu\text{m}$  using an image acquisition system (Spectral Engine 4.0, 4 Pi Analysis Inc., Durham, NC) and image analysis software (SigmaScan-Pro, Jandel Scientific, San Rafael, CA). An energy-dispersive X-ray detector (KEVX 7000, Fisons, San Carlos, CA) was occasionally used to distinguish submicron  $\text{SiO}_2$  particles from the contaminant particles present on the aluminum substrates. Typically, 20-40 SEM fields were acquired across 6 or 7 different magnifications for each sampler. A  $10 \mu\text{m}$  border decision rule was used to handle particles that were only partially within a given SEM field.

The continuous count data were discretized into nine size bins to match those of the impactor. To convert the count data to mass fluxes, values of  $\rho_p = 2.65 \text{ g/cm}^3$ ,  $S_d = 1.36$ , and  $S_v = 1.25$  were used for the particle density, dynamic shape factor, and volume shape factor, respectively. These values were taken from published data presented by Davies (1979) for  $\text{SiO}_2$ . Some degree of particle agglomeration was found in the SEM images, with the agglomerates tending to be more spherical than

the nonagglomerates. Thus the value for  $S_v$  was chosen to be at the upper end of the range of values presented by Davies, i.e., tending towards the more spherical end of the range.

Because  $u_* < 0.4$  m/s for all wind tunnel experiments, Equation (1) was calculated using  $v_{amb} = v_t = \tau g$ , where  $\tau = (\rho_0 d_a^2 C_c)/(18 \mu)$ ,  $\rho_0$  is unit particle density,  $C_c$  is the Cunningham correction factor,  $\mu$  is the dynamic viscosity, and  $g$  is the gravitational acceleration (Wagner and Leith 2001).

## RESULTS

Experimental conditions for the eight wind tunnel experiments are listed in Table 2. Experiments typically lasted 2-8 h. RHs and temperatures ranged from 15 to 50% and 21 to 27 °C, respectively. Aerosol size distributions measured by the impactor were lognormal. Cumulative log-probability plots showed linear relationships, with regression coefficients of  $R^2 \geq 0.99$  for each experiment.

The average number of counts per passive sampler was calculated by dividing the total counts obtained in each experiment by three (Table 2). A typical surface density collected by the passive samplers is shown in Figure 4. Relatively low counts were recorded with the passive samplers because of a limitation imposed by the impactor. Total mass loadings on the impactor substrates of  $>40$  mg led to undesirable amounts of particle bounce, so experiment durations and concentrations had to be kept below certain levels. Evidence of substantial bounce under higher loading conditions included particle deposits in the impactor jets and departures from lognormality in the impactor size distributions. Apparently, collected masses of this magnitude overcame the oleic acid/filter method designed to prevent bounce from occurring. All eight experiments used for analysis had total collected impactor masses of  $<25$  mg.

The mesh factor,  $\gamma_m$ , was determined by comparing impactor concentrations to the averages of the three passive sampler concentrations determined for each experiment. An optimal expression for  $\gamma_m$  was developed by minimizing the sum-of-squares difference between impactor and passive sampler at each size bin, across all experiments. The optimization parameter, OP, was

**Table 2**  
Experimental conditions for passive sampler testing

Test ID	Wind speed (m/s)	Duration (min)	Avg. RH (%)	Avg. temp. (C)	PM10 ( $\text{mg/m}^3$ )*	MMAD ( $\mu\text{m}$ )/GSD*	Avg. count per passive sampler
1	1.5	462	43.2	23.5	1.8	3.1/2.0	60.0
2	1.5	102	14.6	21.5	7.4	2.9/1.9	74.3
3	3	247	16.4	21.1	2.9	2.6/1.7	73.0
4	3	240	22.5	25.6	1.5	2.0/1.8	78.3
5	4	280	50.1	27.0	2.7	2.1/1.5	82.3
6	4	237	15.7	23.0	3.1	2.3/1.8	70.3
7	5	262	20.6	23.3	2.2	2.3/1.8	95.3
8	5	360	30.4	21.8	2.0	2.6/1.9	81.0

\*As measured by the impactor.

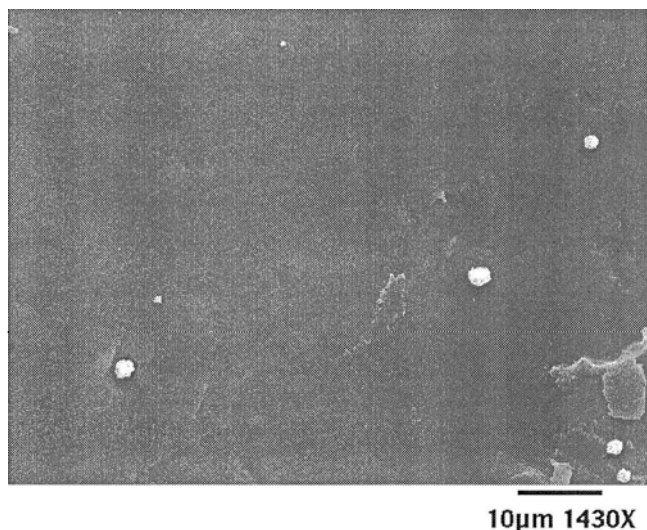


**Figure 4.** SEM image from passive sample analysis.

defined as follows:

$$OP = \sum_{j=1}^8 \left[ \sum_{i=1}^9 \left( \frac{(dC/d \log d_a)_{\text{passive}} - (dC/d \log d_a)_{\text{impactor}}}{(dC/d \log d_a)_{\text{impactor}}} \right)^2 \right]_i \quad [5]$$

where  $(dC/d \log d_a)$  is the concentration of size bin  $i$  (normalized by the width of the bin) and  $j$  is the experiment number. The OP was minimized by formulating  $\gamma_m$  with appropriate dimensionless groups, then determining the constants using the “Solver” tool in Microsoft Excel (Seattle, WA). Data points for which either a) the impactor recorded zero mass or b) the passive sampler average was less than one count per sampler were not included in the optimization. Otherwise, this procedure weighted each size bin equally, independent of the test aerosol’s size distribution.

Several formulations for  $\gamma_m$  were explored, with an emphasis on obtaining the simplest model possible that still provided a good optimization. The following expression was obtained:

$$\begin{cases} \gamma_m = 1, & d_a < 1.63 \mu\text{m}, \\ \gamma_m = (5.95 \times 10^{-3}) Re_p^{-0.439}, & d_a \geq 1.63 \mu\text{m}, \end{cases} \quad [6]$$

where  $Re_p = (d_a v_t / \nu)$ . This relatively simple expression contains one dimensionless group and three parameters, including the diameter at which  $\gamma_m$  starts to steadily decrease with  $d_a$ . Note that this expression is not dependent on  $u_*$  and therefore does not require estimating  $u_*$  when sampling. Only small variations in deposition were observed as a function of wind speed for the experimental conditions ( $u_* < 0.3$  m/s).

Other candidates for  $\gamma_m$  possessed additional parameters and dimensionless groups, including  $u_*$  terms. These models gen-

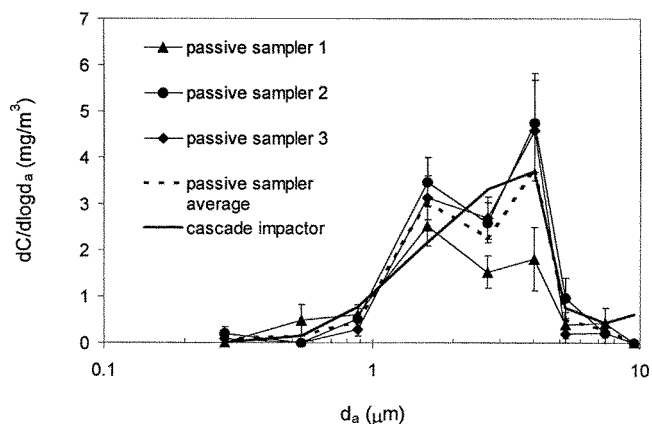


**Figure 5.** Typical results for one experiment: normalized concentration,  $dC/d \log d_a$ , vs. aerodynamic diameter,  $d_a$ , for three passive samplers and an impactor. The average of the three passive samplers’ results is also shown.

erally yielded OP values that were only minor improvements given their added complexity. In addition, these improvements would likely be offset in practice by the uncertainty in estimating  $u_*$ . For these reasons, Equation (6) was judged to be the best expression for  $\gamma_m$ .

Size distributions were then calculated for all experiments using Equations (1) and (6). The results for one experiment are shown in Figure 5. The error bars represent counting error only and were calculated with Poisson statistics.

Figure 6 shows the average passive sampler result for each experiment plotted against the corresponding impactor result. Results are plotted for PM2.5, PM10, mass median aerodynamic diameter (MMAD), and geometric standard deviation (GSD).

To determine sampler precision, a PROC NESTED analysis (SAS, Cary, NC) was performed on the natural logarithms of the passive sampler measurements. This analysis yielded the “within-experiment” variation due to differences among the

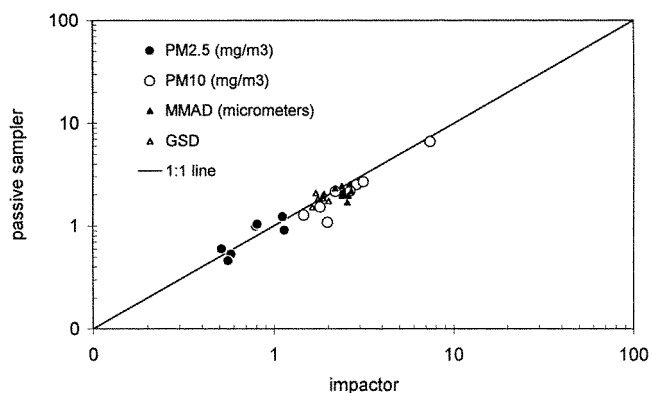


**Figure 6.** PM2.5, PM10, mass median aerodynamic diameter, MMAD, and geometric standard deviation, GSD, as measured by the passive samplers and impactor in the eight wind tunnel experiments.

three samplers in each experiment. The resulting CVs for PM<sub>2.5</sub> and PM<sub>10</sub> were 18.1% and 32.2%, respectively. No consistent patterns were found in the variation between the left, center, and right passive sampler locations. Blank samplers exhibited negligible amounts of SiO<sub>2</sub> for all experiments.

Passive sampler size distributions were found to be approximately lognormal. Regressions for cumulative log-probability plots of the passive results yielded  $R^2 = 0.93\text{--}0.98$ , slightly lower than those determined for the impactor. Because of their lognormality, these size distributions can be adequately summarized in terms of their MMADs and GSDs.

## DISCUSSION

### Accuracy

To evaluate whether accuracy depended on particle size, mass concentration, wind speed, or RH, the results of the three passive samplers in each experiment were averaged. Analysis of variance (ANOVA) was performed on  $\% \text{ error}_{(dC/d \log d_a)}$  to see if particle size was a significant effect. Again, data points that represented an average of  $< 1$  count per sampler were discarded, as were comparisons where zero mass was recorded by the impactor. The dependence of  $\% \text{ error}$  on particle size was found to be insignificant at the 0.05 level ( $p = 0.07$ ).

Wind speed, RH, and concentration were found to be confounders with respect to one other. Thus ANOVA tests performed on each of these quantities were controlled for the other two. ANOVA revealed no significant dependence of  $\% \text{ error}_{\text{PM}_{2.5}}$  and  $\% \text{ error}_{\text{PM}_{10}}$  on wind speed (all  $p$  values  $> 0.5$ ). No dependence of  $\% \text{ error}_{\text{PM}_{2.5}}$  or  $\% \text{ error}_{\text{PM}_{10}}$  was found on impactor PM<sub>10</sub>, the index used for aerosol concentration level (all  $p$  values  $> 0.9$ ). As to be expected with a nonvolatile aerosol, ANOVA showed no significant dependence of these quantities on RH (all  $p$  values  $> 0.6$ ).

No significant variation of  $\% \text{ error}_{\text{MMAD}}$  or  $\% \text{ error}_{\text{GSD}}$  was found with wind speed, concentration level, or RH (all  $p$  values  $> 0.3$ ).

### Precision

As in the previous section, ANOVA tests of wind speed, RH, and concentration were each controlled for the other two. Figure 7 shows CVs for the three passive samplers in each wind tunnel experiment, calculated for PM<sub>2.5</sub> and PM<sub>10</sub> and plotted against wind speed. Although this plot suggests decreasing trends in  $\text{CV}_{\text{PM}_{2.5}}$  and  $\text{CV}_{\text{PM}_{10}}$  with increasing wind speed, these trends are not statistically significant when one controls for concentration and RH (all  $p$  values  $> 0.3$ ). Similarly, the ANOVA tests revealed no significant variation of  $\text{CV}_{\text{PM}_{2.5}}$  or  $\text{CV}_{\text{PM}_{10}}$  on concentration level (all  $p$  values  $> 0.07$ ) or RH (all  $p$  values  $> 0.7$ ).

Some of the between-sampler variation may have been due to small physical differences between each mesh cap. The precision is also dependent on the strength of the analysis technique, which is in turn heavily dependent on counting statistics. Be-

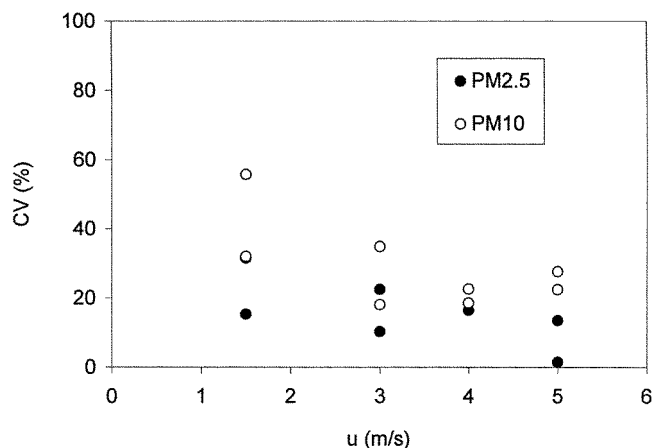


**Figure 7.** Coefficient of variation (CV) of collocated passive samplers for PM<sub>2.5</sub> and PM<sub>10</sub> as a function of wind speed,  $u$ .

cause passive sampler counts were much lower than ideal, the sampler's precision is expected to improve under normal sampling conditions. Even so, the  $\text{CV}_{\text{PM}_{2.5}}$  found here, 18.1%, is comparable to the EPA's stated objective of 15% precision for PM<sub>2.5</sub> samplers (U.S. EPA 1996).

## SENSITIVITY AND UNCERTAINTIES

The sensitivity of passive sampler results to particle density and shape factors was assessed with a representative wind tunnel data set. Table 3 shows the effect of  $\pm 10\%$  changes in  $\rho_p$ ,  $S_d$ , and  $S_v$ , on the average PM<sub>2.5</sub>, PM<sub>10</sub>, MMAD, and GSD. The tabulated numbers represent the average of the changes in the plus and minus directions. The effect of all factors on the GSD was negligible, while the effect of  $\rho_p$  and  $S_d$  on PM<sub>2.5</sub>, PM<sub>10</sub>, and MMAD was  $< 10\%$ . The results were quite sensitive to  $S_v$ , however, as  $\pm 10\%$  changes produced a linear response in MMAD and changes in PM<sub>2.5</sub> and PM<sub>10</sub> of 18 and 21%, respectively. Clearly, one must estimate  $S_v$  accurately. Using the techniques described by Wagner and Leith (2001), one should be able to estimate  $S_v$  to within about 10%.

Semivolatile particles are a potential source of error for the passive sampler. If SEM is used for analysis and the sample is placed under vacuum, the aerosol's volatile components will evaporate. By analyzing only the "dry" component of the aerosol, particle shape factors and densities will be incorrectly assessed and particle size will be underestimated. These errors cause

**Table 3**  
Results of sensitivity analysis

Parameter	Percent change due to $\pm 10\%$ change in parameter:			
	PM <sub>2.5</sub>	PM <sub>10</sub>	MMAD	GSD
$\rho_p$	$\pm 3.6$	$\pm 5.2$	$\pm 6.5$	$\mp 0.5$
$S_d$	$\pm 6.5$	$\pm 4.9$	$\mp 6.5$	$\pm 0.6$
$S_v$	$\pm 18$	$\pm 21$	$\pm 11$	$\mp 0.4$

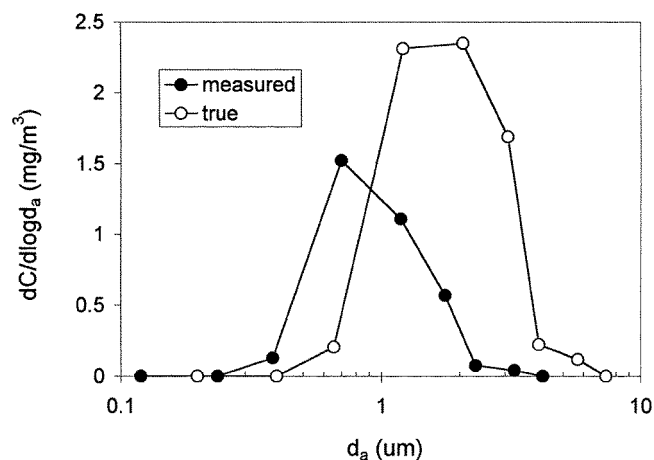


**Figure 8.** Simulated error when sampling an ammonium sulfate aerosol at 90% RH. Normalized concentration,  $dC/d \log d_a$ , vs. aerodynamic diameter,  $d_a$ .

underestimation of both the mass flux and deposition velocity, two deviations which counterbalance each other somewhat.

To assess the consequence of this situation, a sampling simulation was performed in which the particles were assumed to be ammonium sulfate collected at an average RH of 90%. This extreme scenario results in particles that are 75% water by mass. The simulated flux data were then analyzed in two ways. First, an ambient size distribution was calculated using only the dry-component flux, density, and shape factors. Second, a condensation equation accounting for curvature and solute effects (Seinfeld 1986) was used to calculate the "wet" flux at RH = 90%. The wet deposition velocity, density, and shape factors were then used to recalculate the ambient size distribution. The second result represents the "true" distribution, whereas the first represents the inaccurate, "measured" distribution derived from the dry component only (Figure 8). For this simulation, the errors for PM<sub>2.5</sub> and PM<sub>10</sub> are 35 and 47%, respectively. The errors for MMAD and GSD are 46 and 1.5%, respectively. Because this is an extreme scenario, one would obtain much less error under more typical sampling conditions (i.e., lower mean RH or lower volatile aerosol fraction). If ambient-pressure analysis techniques such as atomic force microscopy are used instead of SEM, error would be reduced substantially. Nevertheless, one should be aware of this issue when passively sampling nitrates, organics, or hygroscopic particles. When using SEM, the passive sampler is best suited to applications that do not feature consistently high humidities or aerosols whose mass is dominated by volatile constituents.

These calculations suggest that a nonnegligible degree of measurement error is possible in some cases. However, temporal variability of concentrations is often much larger than these measurement errors (Rappaport 1994). This variability can result in significant errors in conventional long-term averages based on only a few short-term samples. Because the passive sampler effectively integrates over time, it eliminates this source of error and thus long-term averages measured by the passive sampler should generally exhibit better accuracy.

## CONCLUSION

A wind tunnel has been developed to determine the empirical portion of the deposition velocity model and to test the precision of a passive aerosol sampler. The wind tunnel features an aerosol generator that can deliver polydisperse, nonvolatile dusts at high concentrations. The tunnel is relatively small, possessing a straight section 2.4 m long and inner dimensions of (50 × 100) mm. The reference sampler connected to the tunnel, an eight-stage impactor, is equipped with oleic acid-coated filter substrates to minimize particle bounce and an isoaxial, isokinetic probe. Aerosol concentrations were found to have a CV of <6% in the test section, while the diameter of average mass had a CV <1%. Friction velocities were found to range from 0.09 to 0.25 m/s for wind speeds of 1.5 to 5 m/s.

Wind tunnel tests of the passive sampler have determined a sampler precision of  $CV_{PM_{2.5}} = 18.1\%$  and  $CV_{PM_{10}} = 32.2\%$ . The mesh correction factor,  $\gamma_m$ , was empirically determined by minimizing the sum of squares difference between impactor and passive sampler across all size bins and all experiments. The relatively simple correlation is a function of the particle Reynolds number only. ANOVA tests were conducted on accuracy and precision to see whether they depended on wind speed, RH, or aerosol concentration, and accuracy was tested with respect to particle size. No significant trends were observed. The volume shape factor was the most sensitive of the mass and shape conversion variables.

If SEM is used for analysis, the passive sampler will exhibit some error when sampling semivolatile aerosols. For this reason, the passive sampler is probably best suited to applications that do not feature consistently high humidities or aerosols whose mass is dominated by volatile constituents. If ambient-pressure analysis techniques such as atomic force microscopy are used instead of SEM, however, this source of error should be much less. Because the passive sampler integrates over hourly and daily fluctuations in concentration, it should be more accurate than conventional short-term samples when monitoring long-term exposures.

Work is currently underway to test the passive sampler in an occupational setting. These tests will provide a measure of the passive sampler's accuracy under actual, variable conditions.

## ACKNOWLEDGMENTS

The authors wish to thank the National Institute for Occupational Safety and Health (1 R03 OHO3774-01), the U.S. Environmental Protection Agency (U-915321-01-0), the National Institute of Environmental Health Sciences (5 T32 ES07018-21), the U.S. Department of Education (P200A40274-96), and the UNC Board of Governors for supporting this work, Randall Goodman for his assistance with the wind tunnel design, and Dr. Robert Bagnell for his assistance with the SEM analysis.

## REFERENCES

- Davies, C. N. (1979). Particle-Fluid Interaction, *J. Aerosol Sci.* 10:477-513.
- Ramachandran, G., Sreenath, A., and Vincent, J. H. (1998). Towards a New Method for Experimental Determination of Aerosol Sampler Aspiration Efficiency using Scaling Relationships, *J. Aerosol Sci.* 29:875-891.

- Rappaport, S. M. (1994). Interpreting Levels of Exposures to Chemical Agents. In *Patty's Industrial Hygiene and Toxicology, Third Edition, Volume 3, Part A*, edited by R. L. Harris, L. J. Cralley, and L. V. Cralley. John Wiley and Sons, New York, pp. 349–403.
- Schlichting, H. (1979). *Boundary-Layer Theory*, 7th ed., McGraw-Hill, New York, p. 603.
- Seinfeld, J. H. (1986). *Atmospheric Chemistry and Physics of Air Pollution*, John Wiley and Sons, New York, p. 349.
- Turner, J., and Hering, S. (1987). Greased and Oiled Substrates as Bounce Free Impaction Surfaces, *J. Aerosol Sci.* 18:215–224.
- U.S. Environmental Protection Agency (1996). Proposed Requirements for Designation of Reference and Equivalent Methods for PM<sub>2.5</sub> and Ambient Air Quality Surveillance for Particulate Matter, *Fed. Reg.* 61:241, 65785.
- Wagner, J., and Leith, D. (2001). Passive Aerosol Sampler. Part I: Principle of Operation, *Aerosol Sci. Technol.*, (see preceding article in this issue).
- White, F. M. (1994). *Fluid Mechanics*, 3rd ed., McGraw-Hill, New York, p. 314.